INTEGRATED MAGNETIC COMPONENT DESIGN IN SWITCHMODE POWER CONVERTER

Paulo R. T. Rangel
Gerência Educacional de Eletrônica
Centro Federal de Educação Tecnológica de Santa Catarina
Av. Mauro Ramos, 950 – 88020-300 - Florianópolis - SC
phone: (+55 48) 224 0676 fax: (+55 48) 224 0727
prangel@cefetsc.rct-sc.br

João Carlos Fagundes
INEP / EEL / CTC / UFSC
Campus Universitário – Trindade
88040-900 - Florianópolis - SC
phone: (+55)48-3319204 fax: (+55)48-3319280
fagundes@inep.ufsc.br

***Abstract* - This work discusses the analysis and the design of an integrated magnetic component, composed by a transformer and an inductor, both mounted over one single ferrite core, for switchmode power converter applications. The design methodology and the experimental results, considering a single output forward converter are also presented.**

I. INTRODUCTION

Most of the switchmode power converter design requires a high compactation factor, like the ones used in VCR, personal computers, satellite power supply system. One of the main problems in reducing weight, volume and cost is the reduction of the magnetic element size. There are two main possibilities: the increase of the switching frequency to allow the use of smaller magnetic cores, or the integration of inductors and transformers in the same core. The first solution generates some problems, like electromagnetic interference, extra heating of the transistors and magnetic components and low efficiency [1]. The second solution, that uses a single core to build transformers and inductors, allows a low frequency operation and it makes possible a reduction on the weight/volume ratio up to 30%. If it is possible to increase the operation frequency, the integration of the magnetic components allows a higher reduction of them.

Figure 1 shows one of the integration possibilities. In this topology, the transformer effect is represented by the magnetic current flow in the external path, contributing to the energy store in the air gap, placed in the central path, where the inductor is located.

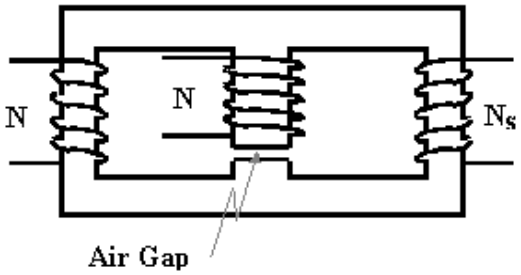

Fig. 1 – Integrated magnetic element.

II. QUALITATIVE ANALYSIS OF THE FORWARD CONVERTER WITH INTEGRATED MAGNETIC ELEMENT

The forward converter, shown in figure 2, is a classical isolated single output. Its input/output voltages transfer function, for continuous conduction mode, is given by the following equation (1):

$$V_o/V_i = D.(N_S/N_{P1}) \qquad (1)$$

where V_i is the input voltage, V_o is the output voltage, N_s and N_{p1} are the turn numbers of secondary and primary windings and D is the cyclic ratio.

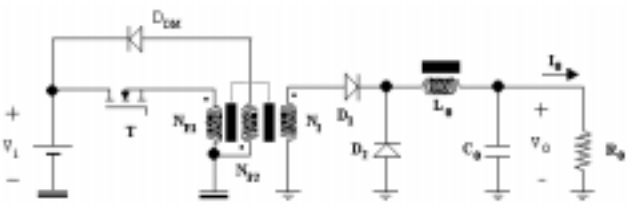

Fig. 2 – Classical isolated single output forward converter.

The ideal transfer function to the forward converter with integrated magnetic element, shown in figure 3, can be obtained by the magnetic flux flowing through the central path of the magnetic element (Φ_L). Due to the AC currents dynamics, this flux is calculated as the difference between the flux produced in the primary side (Φ_P) and the load reaction flux (Φ_S), as shown in figure 4.

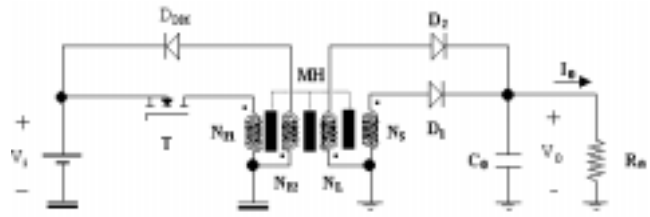

Fig. 3 – Forward converter with integrated magnetic.

The maximum AC flux values are one of the fundamental factors to the core selection, due the forward transistor switching and the load current. The flux caused

by the transistor switching goes to maximum value in $D.T_S$ instant, where T_S is the switching period. Then, it is possible to write:

$$\Delta\Phi_P = (V_i.D.T_S)/N_{P1} \quad (2)$$

where $\Delta\Phi_P$ is the magnetic flux variation in the primary side.

The load reaction creates a maximum flux variation, evaluated as:

$$\Delta\Phi_S = (V_o.D.T_S)/N_S \quad (3)$$

where $\Delta\Phi_S$ is the magnetic flux variation in the secondary side.

Since the difference between these two fluxes components should circulate through the central path and considering that $N_L = N_S$ to avoid a quick decrease of the output current, it is possible to write:

$$\Delta\Phi_L = (V_o.\ D'.\ T_S)/N_S \quad (4)$$

Where $\Delta\Phi_L$ is the flux variation in the central path.

With:

$$\Delta\Phi_L = \Delta\Phi_P - \Delta\Phi_S \quad (5)$$

From equations (4) and (5), it is possible to obtain the same transfer function shown in (1), indicating that the operation of this converter is similar for the classical forward converter.

III. Integrated Magnetic Element for Forward Converters

The analysis of the integrated magnetic element for a forward converter with a single output should preview the DC bias question. The central path will see more flux bias than the external path due the energy stored in the air gap. The bias flux in the inductor of the integrated magnetic element should be the same of the flux in a conventional inductor. So, the placement of the transformer windings should not ideally add any DC bias effect.

Figure 4 shows an electric equivalent circuit where the air gap reluctance (R_{EF}) is much bigger than the core magnetic reluctance (Rn) which will be used to model the magnetic circuit.

It is possible to determine that the DC bias flux flowing through the external path has the half part of the flux flowing through the central path, due the core E-I symmetry, as shown in [1].

$$\Phi_S = \Phi_P = 0{,}5.\Phi_L \quad (6)$$

where Φ_P and Φ_S are the magnetic flux in the primary and in secondary, respectively, and Φ_L is the magnetic flux in the central path.

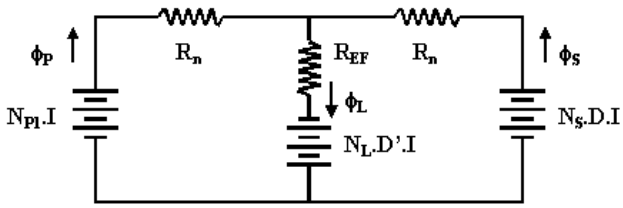

R_n – magnetic reluctance of the external path;
R_{EF} - magnetic reluctance of the air gap;
$N_{P1}.I_P$ – primary MMF;
$N_L.D'.I_0$ – MMF generated by the inductor;
$N_S.D.I_0$ – secondary MMF;
D'= 1-D, where D is the duty cycle.

Fig. 4 – Equivalent circuit to DC bias flux analysis.

Considering that the AC flux is higher than the polarization flux, the total magnetic flux in each path can be calculated by:

$$\Phi_{Pmáx} = (V_o.T_S)/(2.N_S) + 0{,}5.\Phi_L \quad (7)$$

$$\Phi_{Lmáx} = (V_o.D'.T_S)/(2.N_S) + \Phi_L \quad (8)$$

$$\Phi_{Smáx} = (V_o.D.T_S)/(2.N_S) + 0{,}5.\Phi_L \quad (9)$$

where Φ_{PMAX} and Φ_{SMAX} are the maximum magnetic flux in the primary and in the secondary, respectively, and Φ_{LMAX} is the maximum magnetic flux in the central path.

IV. Design Methodology

Knowing the maximum values of the magnetic flux through the external and central path and the maximum flux density, it is possible to define the core area relations [1]. Then:

$$A = \Phi_{máx}/B_{máx} \quad (10)$$

$$A_{P/L} = (0{,}5 + \Delta I_o/I_o)/(1 + 0{,}5.\ \Delta I_o/I_o) \quad (11)$$

$$A_{S/L} = (0{,}5.\ \Delta I_o/I_o + 0{,}5)/(1 + 0{,}5.\ \Delta I_o/I_o) \quad (12)$$

The core geometry factor contributes effectively to the calculation of the weight and volume savings [2].

$$W = A'.Kg^{0,6} \quad (13)$$

$$V = A.Kg^{0,6} \quad (14)$$

where W is the weight, V is the volume, Kg is the geometry factor, A and A' are proportional factors, which are dependents on the shape and composition of the magnetic material used in the core.

In addition, the geometry factor, the electrical losses in the core, the occupation of the windows by the windings and the gap length can be defined [1], [2].

V. Experimental Results

In order to validate the analytical studies a prototype was built, considering a single ended forward converter,

composed by an integrated magnetic element and with the following specifications:

Output power (P_o): 100W
Input voltage (V_i): 220V
Output voltage (V_o): 15V
Output current (I_o): 6.67A
Ripple voltage (ΔV_o): ± 100mV
Efficiency (η): 75%
Switching frequency (f_S): 100kHz

The aim of this procedure is to verify the converter behavior, identifying the advantages and eventual disadvantages of this topology in comparison with the conventional converter using discrete magnetic elements.

Figure 5 shows the regulation of the converter considering an input voltage variation of ± 20V.

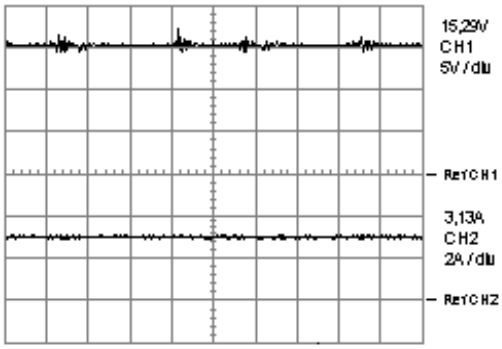

(a)

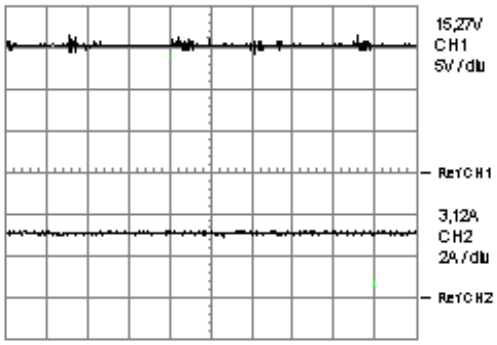

(b)

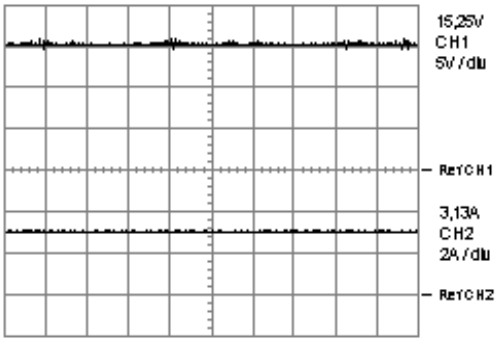

(c)

Fig. 5 – Output voltage and current to (a) Vin=220V, (b) Vin=200V e (c) Vin = 240V.

Figure 6(a) shows the primary side and demagnetization winding voltages, figure 6(b) shows the secondary side voltage and figure 6(c) shows the inductor voltage.

In figure 7 the full load operation is shown.

It is possible to verify by the observation of the wave shape presented previously, that the integrated magnetic element has the same behavior of the discrete magnetic elements of the classic converter. The output voltage and the output current have a good performance, but it can be improved by reducing the noise using filters and a optimized layout of the PCB.

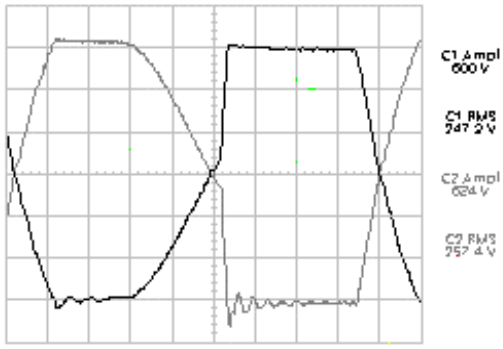

(a)

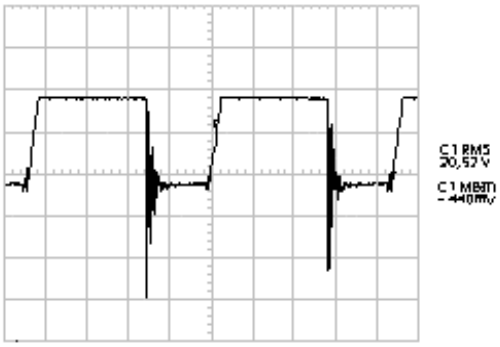

(b)

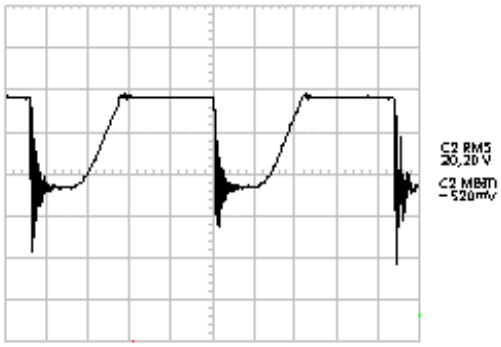

(c)

Fig. 6 – Voltage on: (a) primary side and demagnetization winding; (b) secondary side and (c) inductor.

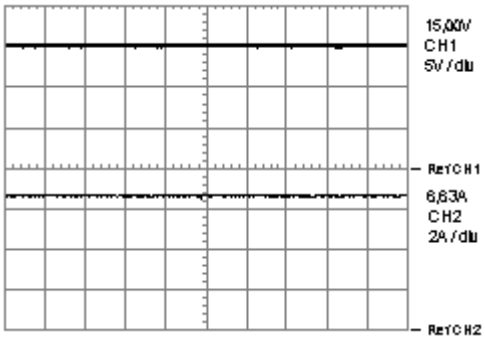

Fig. 7 – Full load voltage and amperage

The impact of the adopted design methodology in the volume reduction can be calculated comparing the total volume occupied by the discrete transformer and inductor and the volume of the integrated magnetic element. In the first case it is necessary a EE42/15 and a EEL28 magnetic cores, for the transformer and inductor, respectively . For the integrated magnetic component it is necessary a EC52 core. Both cores are manufactured by THORNTON and their correspondent volume are:

EE42/15: 17600mm^3
EEL28: 6344mm^3
EC52: 18800mm^3

The volume reduction obtained in this case is about 21.5%.

Figure 8 shows the prototype built with the specifications previously presented.

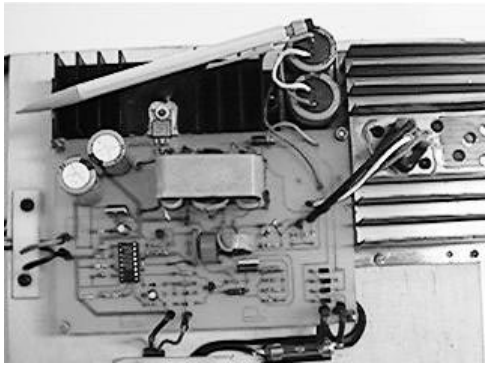

Fig. 8 – Prototype of a forward converter with integrated magnetic component.

VI. Conclusions

The main contribution of this paper in the study of the integrated magnetic elements use is the determination of a simple and easy methodology allowing an immediately application in power supply design.

It was shown in this paper that, comparing the design, construction and analysis of the forward converter with integrated magnetic element to the classic forward converter, there is a real possibility of weight and volume reduction of the magnetic elements. Considering the availability of commercial magnetic cores this reduction is around 10% and 25%.

The construction of the integrated magnetic element and its weight/volume ratio can be optimized more efficiently if considering the possibility of use of a special designed core.

VII. References

[1] Ed Bloom, “Core selection for & design aspects of an integrated-magnetic forward converter”, in *Proceedings of the Power Electronics Specialists Conference*, 1996, pp.141-150.

[2] Colonel Wm. T. McLyman, *Magnetic core selection for transformers and inductors*, Marcel Dekker, inc. New York, USA, 1982.

[3] Arthur F. Witulski, “Introduction to modeling of transformers and coupled inductors”, *IEEE Transactions on Power Electronics*, Vol. 10, nº 3, May 1995.

[4] J. A. Basset, “Constant frequency ZVS converter with integrated magnetics”, IEEE, 1992.